J|A|C|S ARTICLES

Published on Web 04/23/2009

Dioxygen and Water Activation Processes on Multi-Ru-Substituted Polyoxometalates: Comparison with the "Blue-Dimer" Water Oxidation Catalyst

Aleksey E. Kuznetsov, Yurii V. Geletii, Craig L. Hill, Keiji Morokuma, and Djamaladdin G. Musaev*

Cherry L. Emerson Center for Scientific Computation and Department of Chemistry, Emory University, 1515 Dickey Drive, Atlanta, Georgia 30322

Received January 2, 2009; E-mail: dmusaev@emory.edu

Abstract: Dioxygen and water activation on multi-Ru-substituted polyoxometalates were studied using the B3LYP density functional method. It was shown that the reaction of the Ru_2-substituted γ-Keggin polyoxotungstate $\{\gamma\text{-}[(H_2O)Ru^{III}(\mu\text{-}OH)_2Ru^{III}(H_2O)][SiW_{10}O_{36}]\}^{4-}$, **I($H_2O$)**, with O_2 is a 4-electron highly exothermic [$\Delta E_{gas} = 62.5$ ($\Delta E_{gas} + \Delta G_{solv(water)} = 24.6$) kcal/mol] process and leads to formation of $(H_2O)\{\gamma\text{-}[(O)Ru(\mu\text{-}OH)_2Ru(O)](H_2O)[SiW_{10}O_{36}]\}^{4-}$, **IV($H_2O$)**. Both the stepwise (or dissociative) and the concerted (or associative) pathways of this reaction occurring with and without water dissociation, respectively, were examined, and the latter has been found to be kinetically more favorable. It was shown that the first 1e-oxidation is achieved by the H_2O-to-O_2 substitution, which might occur with a maximum of 23.1 (10.5) kcal/mol barrier and leads to the formation of $\{\gamma\text{-}[(OO)Ru(\mu\text{-}OH)_2Ru(H_2O)](H_2O)[SiW_{10}O_{36}]\}^{4-}$, **II($H_2O$)**. The second 1e-oxidation is initiated by the proton transfer from the coordinated water molecule to the superoxide (OO^-) ligand in **II(H_2O)** and is completed upon formation of hydroperoxo−hydroxo intermediate $\{\gamma\text{-}[(OOH)Ru(\mu\text{-}OH)_2Ru(OH)](H_2O)[SiW_{10}O_{36}]\}^{4-}$, **III-1($H_2O$)**. The final 2e-oxidation occurs upon the proton transfer from the terminal OH-ligand to the Ru-coordinated OOH fragment and is completed at the formation of $(H_2O)\cdots\{\gamma\text{-}[(O)Ru(\mu\text{-}OH)_2Ru(O)](H_2O)[SiW_{10}O_{36}]\}^{4-}$, **IV($H_2O$)**, with two Ru=O bonds. Each step in the associative pathway is exothermic and occurs with small energy barriers. During the process, the oxidation state of Ru centers increases from +3 to +4. The resulting **IV(H_2O)** with a $\{Ru(O)(\mu\text{-}OH)_2Ru(O)\}$ core should be formulated to have the Ru^{IV}=$O^{\bullet}$ units, rather than the Ru^{V}=O groups. The reverse reaction, water oxidation by **IV(H_2O)**, is found to be highly endothermic and cannot occur; this finding is different from that reported for the "blue-dimer" intermediate, $\{(bpy)_2[(O^{\bullet})Ru(\mu\text{-}O)Ru(O^{\bullet})](bpy)_2\}^{4+}$, which readily oxidized an incoming water molecule to produce O_2.[2,29−40,60−62] The main reason for this difference in reactivity of **IV(H_2O)** (i.e., Ru_2−POM) and the "blue-dimer" intermediates toward the water molecule is found to be a high stability of **IV(H_2O)** as compared to the analogous "blue-dimer" intermediate relative to O_2 formation. This, in turn, derives from the electron-rich nature of $[SiW_{10}O_{36}]^{4-}$ as compared to bpy ligands.

I. Introduction

The development of reactive, selective, stable, and well-defined molecular catalysts for water oxidation is of intellectual and potential practical importance in artificial photosynthesis (solar driven splitting of H_2O).[1−28] High-resolution crystal structures of the photosystem II, Nature's efficient water oxidation system, have revealed the Mn_4Ca-core oxygen-evolving center (OEC) in this biological system.[9−17] Numerous studies of model compounds have provided insight into the properties of this multimetal biocatalyst.[6,11,18−24] Parallel efforts led to several biomimetic clusters of transition metals that catalyze water oxidation.[29−41] Among these early findings, the "blue-dimer", $[(bpy)_2(H_2O)Ru(\mu\text{-}O)Ru(H_2O)(bpy)_2]^{4+}$,[2] discovered by Meyer and co-workers, has attracted considerable

(1) Shafirovich, V. Y.; Khannanov, N. K.; Strelets, V. V. *Nouv. J. Chim.* **1980**, *4*, 81–84.
(2) Gersten, S. W.; Samuels, G. J.; Meyer, T. J. *J. Am. Chem. Soc.* **1982**, *104*, 4029–4030.
(3) Rotzinger, F. P.; Munavalli, S.; Comte, P.; Hurst, J. K.; Grätzel, M.; Pern, F.-J.; Frank, A. J. *J. Am. Chem. Soc.* **1987**, *109*, 6619–6626.
(4) Meyer, T. J. *Acc. Chem. Res.* **1989**, *22*, 163–170.
(5) Rüttinger, W.; Dismukes, G. C. *Chem. Rev.* **1997**, *97*, 1–24.
(6) Limburg, J.; Vrettos, J. S.; Liable-Sands, L. M.; Rheingold, A. L.; Crabtree, R. H.; Brudvig, G. W. *Science* **1999**, *283*, 1524–1527.
(7) Hara, M.; Waraksa, C. C.; Lean, J. T.; Lewis, B. A.; Mallouk, T. E. *J. Phys. Chem. A* **2000**, *104*, 5275–5280.
(8) Grätzel, M. *Nature (London)* **2001**, *414*, 338–344.
(9) Yagi, M.; Kaneko, M. *Chem. Rev.* **2001**, *101*, 21–35.
(10) Yachandra, V. K.; Sauer, K.; Klein, M. P. *Chem. Rev.* **1996**, *96*, 2927–2950.
(11) Mukhopadhyay, S.; Mandal, S. K.; Bhaduri, S.; Armstrong, W. H. *Chem. Rev.* **2004**, *104*, 3981–4026.
(12) Zouni, A.; Witt, H.-T.; Kern, J.; Fromme, P.; Krauss, N.; Saenger, W.; Orth, P. *Nature (London)* **2001**, *409*, 739–743.
(13) Kamiya, N.; Shen, J.-R. *Proc. Natl. Acad. Sci. U.S.A.* **2003**, *100*, 98–103.
(14) Biesiadka, J.; Loll, B.; Kern, J.; Irrgang, K.-D.; Zouni, A. *Phys. Chem. Chem. Phys.* **2004**, *6*, 4733–4736.
(15) Loll, B.; Kern, J.; Saenger, W.; Zouni, A.; Biesiadka, J. *Nature (London)* **2005**, *438*, 1040–1044.
(16) McEvoy, J. P.; Brudvig, G. W. *Chem. Rev.* **2006**, *106*, 4455–4483.
(17) Yano, J.; Yachandra, V. K. *Inorg. Chem.* **2008**, *47*, 1711–1726.
(18) Limburg, J.; Vrettos, J. S.; Chen, H.; de Paula, J. C.; Crabtree, R. H.; Brudvig, G. W. *J. Am. Chem. Soc.* **2001**, *123*, 423–430.

10.1021/ja900017g CCC: $40.75

attention.[29−35,39,41] These extensive studies have elucidated some mechanistic aspects of water oxidation, pointed out key challenges, and highlighted the intrinsic limitation of catalysts having organic ligands. These ligands are thermodynamically unstable to oxidation by O_2 and more potent oxidants with respect to CO_2 and H_2O and react rapidly and irreversibly with well-known intermediates in H_2O oxidation rendering such ligands problematic for practical water oxidation catalysts.[2,5,6,11,29,33,34,39] Thus, the need to design highly active and stable H_2O oxidation catalysts remains of central importance. On the basis of (a) the reports on the "blue-dimer" catalyst for H_2O oxidation, (b) polyoxometalate (POM) complexes with multinuclear d-electron-containing centers capable of accepting several electrons needed for H_2O oxidation,[42−55] and (c) the report by Shannon and coworkers on the electrocatalytic O_2 generation by the Neumann−Khenkin complex, $[WZnRu_2(OH)(H_2O)(ZnW_9O_{34})_2]^{11-}$,[56] we predicted and prepared[57] $[\{Ru^{III}_2(OH)_2\}(\gamma\text{-}SiW_{10}O_{36})]^{4-}$ (**1**) complex, which oxidizes in aqueous solution to give $Rb_8K_2[\{Ru_4O_4(OH)_2(H_2O)_4\}(\gamma\text{-}SiW_{10}O_{36})_2]\cdot 25H_2O$ (**2**). The latter is an oxidatively and hydrolytically stable compound that catalyzes the rapid oxidation of H_2O to O_2 in aqueous solution at pH 7 and is quite stable under turnover conditions.[58] Independently and simultaneously, a group of scientists from the Universities of Padova and Trieste (Italy) and Princeton (U.S.) prepared a very similar complex (different counterions) using a different route and documented that it catalyzed H_2O oxidation by Ce(IV) in strong aqueous acid (pH $\approx$ 1).[59]

Our previous computational studies[58] demonstrated that the reaction of $[\{Ru^{III}_2(OH)_2\}(\gamma\text{-}SiW_{10}O_{36})]^{4-}$, **1**, with O_2, **1** + O_2 → $[\{Ru^{V}_2(O)_2(OH)_2\}(\gamma\text{-}SiW_{10}O_{36})]^{4-}$ (**3**), is an exothermic process, suggesting the feasibility of O−O bond activation by the dihydroxo-bridged di-Ru^{III} unit inside the inorganic POM framework. This finding is diametrically opposite from the conclusions of numerous studies on the water oxidation by the "blue-dimer".[29,33,39,60−62] For instance, from the work by Yang and Baik,[39] one may conclude that the reaction of $[(bpy)_2(H_2O)Ru^{III}-(\mu\text{-}O)-Ru^{III}(H_2O)(bpy)_2]^{4+}$ with O_2 to produce a complex with an $\{(O)Ru-(\mu\text{-}O)-Ru(O)\}$ core is endothermic by 22.8 kcal/mol and occurs with a large (48.7 kcal/mol) energy barrier. Similarly, our studies show (see below) that complex **3** cannot facilitate water oxidation. However, previous investigations, both experimental and theoretical,[2,5,29−35,39,41,60−62] have shown that water oxidation by $[(bpy)_2(O)Ru^{V}-(\mu\text{-}O)-Ru^{V}(O)(bpy)_2]^{4+}$ is a facile process. Yang and Baik[39] have shown that the reaction of $[(bpy)_2(O)Ru^{V}-(\mu\text{-}O)-Ru^{V}(O)(bpy)_2]^{4+}$ with water produces a hydroperoxo−hydroxo intermediate $\{(HOO)Ru^{IV}-(\mu\text{-}O)-Ru^{IV}(OH)\}$, which later transforms to peroxo-aqua intermediates with $\{(O_2)Ru^{IV}-(\mu\text{-}O)-Ru^{IV}(H_2O)\}$ and $\{(O_2)Ru^{IV}-(\mu\text{-}O)-Ru^{III}(H_2O)\}$ cores. The latter species interacts with another H_2O molecule to produce a triplet O_2 molecule (which contains one O atom from a solvent water molecule and one O atom from the di-Ru-complex) and the original complex $[(bpy)_2(H_2O)Ru^{III}-(\mu\text{-}O)-Ru^{III}(H_2O)(bpy)_2]^{4+}$. The computed rate-determining activation barrier of 25.9 kcal/mol, which corresponds to the step for formation of the hydroperoxo−hydroxo intermediate, is in good agreement with the experimentally estimated

(19) Chen, H.; Tagore, R.; Olack, G.; Vrettos, J. S.; Weng, T.-C.; Penner-Hahn, J.; Crabtree, R. H.; Brudvig, G. W. *Inorg. Chem.* **2007**, *46*, 34–43.
(20) Tagore, R.; Chen, H.; Zhang, H.; Crabtree, R. H.; Brudvig, G. W. *Inorg. Chim. Acta* **2007**, *360*, 2983–2989.
(21) Carrell, T. G.; Cohen, S.; Dismukes, G. C. *J. Mol. Catal. A* **2002**, *187*, 3–15.
(22) Chen, H.; Faller, J. W.; Crabtree, R. H.; Brudvig, G. W. *J. Am. Chem. Soc.* **2004**, *126*, 7345–7349.
(23) Tagore, R.; Crabtree, R. H.; Brudvig, G. W. *Inorg. Chem.* **2008**, *47*, 1815–1823.
(24) Pecoraro, V. L.; Hsieh, W.-Y. *Inorg. Chem.* **2008**, *47*, 1765–1778.
(25) Betley, T. A.; Surendranath, Y.; Childress, M. V.; Alliger, G. E.; Fu, R.; Cummins, C. C.; Nocera, D. G. *Philos. Trans. R. Soc. London, Ser. B* **2008**, *363*, 1293–1303.
(26) Lewis, N. S.; Nocera, D. G. *Proc. Natl. Acad. Sci. U.S.A.* **2006**, *103*, 15729–15735.
(27) Kanan, M. W.; Nocera, D. G. *Science* **2008**, *321*, 1072–1075.
(28) Betley, T. A.; Wu, Q.; Voorhis, T. V.; Nocera, D. G. *Inorg. Chem.* **2008**, *47*, 1849–1861.
(29) Liu, F.; Concepcion, J. J.; Jurss, J. W.; Cardolaccia, T.; Templeton, J. L.; Meyer, T. J. *Inorg. Chem.* **2008**, *47*, 1727–1752.
(30) Alstrum-Acevedo, J. H.; Brennmann, M. K.; Meyer, T. J. *Inorg. Chem.* **2005**, *44*, 6802–6827.
(31) Huynh, M. H. V.; Meyer, T. J. *Chem. Rev.* **2007**, *107*, 5004–5064.
(32) Huynh, M. H. V.; Dattelbaum, D. M.; Meyer, T. J. *Coord. Chem. Rev.* **2005**, *249*, 457–483.
(33) Hurst, J. K.; Cape, J. L.; Clark, A. E.; Das, S.; Qin, C. *Inorg. Chem.* **2008**, *47*, 1753–1764.
(34) Hurst, J. K. *Coord. Chem. Rev.* **2005**, *249*, 313–328.
(35) Romero, I.; Rodriguez, M.; Sens, C.; Mola, J.; Kollipara, M. R.; Francàs, L.; Mas-Marza, E.; Escriche, L.; Llobet, A. *Inorg. Chem.* **2008**, *47*, 1824–1834.
(36) Deng, Z.; Tseng, H.-W.; Zong, R.; Wang, D.; Thummel, R. *Inorg. Chem.* **2008**, *47*, 1835–1848.
(37) Zong, R.; Thummel, R. *J. Am. Chem. Soc.* **2005**, *127*, 12802–12803.
(38) Muckerman, J. T.; Polyanski, D. E.; Wada, T.; Tanaka, K.; Fujita, E. *Inorg. Chem.* **2008**, *47*, 1787–1802.
(39) Yang, X.; Baik, M.-H. *J. Am. Chem. Soc.* **2006**, *128*, 7476–7485.
(40) Liu, F.; Cardolaccia, T.; Hornstein, B. J.; Schoonover, J. R.; Meyer, T. J. *J. Am. Chem. Soc.* **2007**, *129*, 2446–2447.
(41) Süss-Fink, G. *Angew. Chem., Int. Ed.* **2008**, *47*, 5888–5890.
(42) Pope, M. T.; Müller, A. *Angew. Chem., Int. Ed.* **1991**, *30*, 34–48.
(43) Borrás-Almenar, J. J.; Coronado, E. ; Müller, A.; Pope, M. T. *Polyoxometalate Molecular Science*; Kluwer Academic Publishers: Dordrecht, 2003; Vol. 98.
(44) Pope, M. T. In *Comprehensive Coordination Chemistry-II: From Biology to Nanotechnology*; Wedd, A. G., Ed.; Elsevier Ltd.: Oxford, UK, 2004; Vol. 4, pp 635−678.
(45) Hill, C. L. In *Comprehensive Coordination Chemistry-II: From Biology to Nanotechnology*; Wedd, A. G., Ed.; Elsevier Ltd.: Oxford, UK, 2004; Vol. 4, pp 679−759.
(46) Hill, C. L.; Prosser-McCartha, C. M. *Coord. Chem. Rev.* **1995**, *143*, 407–455.
(47) Okuhara, T.; Mizuno, N.; Misono, M. *Adv. Catal.* **1996**, *41*, 113–252.
(48) Neumann, R. *Prog. Inorg. Chem.* **1998**, *47*, 317–370.
(49) Neumann, R. In *Modern Oxidation Methods*; Bäckvall, J. E., Ed.; Wiley-VCH: Weinheim, 2004; pp 223−251.
(50) Mizuno, N.; Yamaguchi, K.; Kamata, K. *Coord. Chem. Rev.* **2005**, *249*, 1944–1956.
(51) Keita, B.; Mbomekalle, I. M.; Lu, Y. W.; Nadjo, L.; Berthet, P.; Anderson, T. M.; Hill, C. L. *Eur. J. Inorg. Chem.* **2004**, 3462–3475.
(52) Keita, B.; Mbomekalle, I. M.; Nadjo, L.; Anderson, T. M.; Hill, C. L. *Inorg. Chem.* **2004**, *43*, 3257–3263.
(53) Anderson, T. M.; Cao, R.; Neiwert, W. A.; Hardcastle, K. I.; Hill, C. L.; Ammam, M.; Keita, B.; Nadjo, L. *Eur. J. Inorg. Chem.* **2005**, 1770–1775.
(54) Keita, B.; Mialane, P.; Sécheresse, F.; de Oliveira, P.; Nadjo, L. *Electrochem. Commun.* **2007**, *9*, 164–172.
(55) Sadakane, M.; Tsukuma, D.; Dickman, M. H.; Bassil, B. S.; Kortz, U.; Capron, M.; Ueda, W. *Dalton Trans.* **2007**, 2833–2838.
(56) Howells, A. R.; Sankarraj, A.; Shannon, C. *J. Am. Chem. Soc.* **2004**, *126*, 12258–12259.
(57) Quiñonero, D.; Wang, Y.; Morokuma, K.; Khavrutskii, L. A.; Botar, B.; Geletii, Y. V.; Hill, C. L.; Musaev, D. G. *J. Phys. Chem. B* **2006**, *110*, 170–173.
(58) Geletii, Y.; Botar, B.; Kögerler, P.; Hillesheim, D. A.; Musaev, D. G.; Hill, C. L. *Angew. Chem., Int. Ed.* **2008**, *47*, 3896–3899.
(59) Sartorel, A.; Carraro, M.; Scorrano, G.; Zorzi, R. D.; Geremia, S.; McDaniel, N. D.; Bernhard, S.; Bonchio, M. *J. Am. Chem. Soc.* **2008**, *130*, 5006–5007.
(60) Bartolotti, L. J.; Pedersen, L. G.; Meyer, T. J. *Int. J. Quantum Chem.* **2001**, *83*, 143–149.
(61) Yang, X.; Baik, M.-H. *J. Am. Chem. Soc.* **2004**, *126*, 13222–13223.
(62) Batista, E. R.; Martin, R. L. *J. Am. Chem. Soc.* **2007**, *129*, 7224–7225.

value of 18.7−23.3 kcal/mol.[39,63] Thus, the bridged di-Ru systems placed in different ligand environments exhibit different reactivity toward O_2; the μ-oxo-bridged di-Ru unit ligated by small organic moieties is capable of water oxidation but not of O−O bond activation. In contrast, the di-μ-hydroxo-bridged di-Ru^{III} unit ligated by the large inorganic polyoxometalate moiety (as in complex **1**) is capable of the O−O bond activation but not water oxidation.

To defensibly rationalize the above-reported difference in the reactivity of **1** and the "blue-dimer" toward dioxygen, in this Article we computationally studied the mechanism and governing factors in O−O bond activation by **1**, and we compare our findings with analogous results of Baik and co-workers[39] on the reaction of the "blue-dimer" with O_2. We hope that this strategy will allow us to elucidate the reasons for the observed difference in the reactivity of **1** and $[(bpy)_2(H_2O)Ru^{III}-(\mu\text{-}O)-Ru^{III}(H_2O)(bpy)_2]^{4+}$ toward the dioxygen molecule.

II. Computational Details

All calculations were performed using the Gaussian 03 program.[64] The geometries of all species under investigation were optimized without any symmetry constraint at the B3LYP/Lanl2dz level of theory with additional d polarization functions for the Si atom ($\alpha = 0.55$) and the corresponding Hay−Wadt effective core potentials (ECPs) for W and Ru.[65−70] This method is subsequently referred to as "B3LYP/[Lanl2dz + d(Si)]". The energetics of the optimized structures were further refined by performing single-point calculations using the Stuttgart group's pseudopotentials[71] and associated SDD basis sets for W and Ru and the standard 6-31+G* split-valence-polarization basis set for all other atoms. This method will be subsequently referred to as "B3LYP/SDD".

Antiferromagnetic exchange coupling constants (J) as well as its contribution to the energy of the broken symmetry state of the reported structures were calculated by utilizing the Yamaguchi−Noodleman approach.[72]

Only for transition states, Hessians were calculated and confirmed to have one imaginary frequency corresponding to the reaction coordinates. The solvent effects were estimated at the B3LYP/SDD level of theory using the self-consistent reaction field IEF-PCM method[73] (UAKS model) with water as a solvent (dielectric constant $\varepsilon = 78.39$). Below, we discuss gas-phase energetics ΔE (without zero point correction) calculated at the B3LYP/SDD level of theory. The energies including solvent effects $\Delta E + \Delta G_{solv}$ are provided in parentheses. The Cartesian coordinates of all optimized structures at the B3LYP/[Lanl2dz + d(Si)] level along with the results of their Mulliken analysis are presented in the Supporting Information (Tables S1 and S2, respectively). An overall charge of the studied species is chosen to be "4−".

One should note that, as it could be expected, about 88−90% of PCM contribution to energy is due to electrostatic interactions between the solute and solvent. Nonelectrostatic components of this energy (including cavitation, dispersion, and repulsion energies) are only within 12−10% for all of the calculated structures (see Table S3 of the Supporting Information).

III. Results and Discussion

A. Geometry and Electronic Structure of the Reactant. As expected, the prereaction complex in aqueous solution is a bis-aqua complex $\{\gamma\text{-}[(H_2O)Ru^{III}-(\mu\text{-}OH)_2-Ru^{III}(H_2O)][SiW_{10}O_{36}]\}^{4-}$, **I(H$_2$O)**, which is formed by adding two water molecules to $\{\gamma\text{-}[Ru^{III}-(\mu\text{-}OH)_2-Ru^{III}][SiW_{10}O_{36}]\}^{4-}$, **1**. The geometry and electronic structure of complex **1** were the subject of our previous papers.[57,74] Briefly, it was found that **1** has a singlet ground electronic state with the calculated Ru−Ru, $Ru-O^5/O^6$, $Ru-O_{Si}$, and $Ru-O^7/O^8$ bond distances of 2.60, 2.08, 2.05, and 1.98 Å, respectively. In general, water molecules can coordinate to Ru-atoms of **1** in several different ways leading to multiple isomers of bis-aqua complex **I(H$_2$O)**. We have exhaustively explored several structural isomers of **I(H$_2$O)** in their different lower-lying spin states. Here, we discuss only the energetically most stable isomer of **I(H$_2$O)**. The most important geometry parameters of **I(H$_2$O)** are given in Figure 1, while its Cartesian coordinates and full results of Mulliken analysis are provided in the Supporting Information.

Calculations show that addition of two water molecules does not change the ground electronic state of complex **1**; the ground electronic state of the resulting complex **I(H$_2$O)** is also a singlet state. One should note that for the $\{(bpy)_2[(H_2O)Ru^{III}-(\mu\text{-}O)-Ru^{III}(OH_2)](bpy)_2\}^{4+}$ complex Yang and Baik[39] have reported the high-spin ground electronic state, while the antiferromagnetically coupled open-shell singlet state was reported to be only 5.7 kcal/mol higher. As seen in Figure 1, in **I(H$_2$O)**, water molecules form hydrogen bonds with OH and O (located between Ru and W atoms) centers of the POM. The calculated Ru^1-O^1, O^5-H^1, O^6-H^2, Ru^2-O^2, O^7-H^3, and O^8-H^4 bond distances are 2.19, 2.01, 2.02, 2.28, 2.08, and 2.06 Å, respectively. These $Ru-O_{(H_2O)}$ bond distances, 2.19 and 2.28 Å, lie well within the range of $M-O_{(H_2O)}$ bond distances found for other POM compounds[75−80] and late-transition metal oxo complexes.[81,82] Comparison of the important geometry parameters of **I(H$_2$O)** and **1** (presented above) shows that coordination of water molecules to POM only changes the Ru−Ru, $Ru-O^5/O^6$, and $Ru-O^7/O^8$ bond distances slightly. The most noteworthy geometry change is elongation of the $Ru-O_{Si}$ bond distances, from 2.07 and 2.07 Å in **1** to 2.10 and 2.12 Å in **I(H$_2$O)**. Despite

(63) Yamada, H.; Siems, W. F.; Koike, T.; Hurst, J. K. *J. Am. Chem. Soc.* **2004**, *126*, 9786–9795.
(64) Frisch, M. J.; et al. *Gaussian 03*, revision C1; Gaussian, Inc.: Wallingford, CT, 2004.
(65) Becke, A. D. *Phys. Rev. A* **1988**, *38*, 3098–3107.
(66) Lee, C.; Yang, W.; Parr, R. G. *Phys. Rev. B* **1988**, *37*, 785–789.
(67) Becke, A. D. *J. Chem. Phys.* **1993**, *98*, 1372–1380.
(68) Hay, P. J.; Wadt, W. R. *J. Chem. Phys.* **1985**, *82*, 270–283.
(69) Hay, P. J.; Wadt, W. R. *J. Chem. Phys.* **1985**, *82*, 299–310.
(70) Wadt, W. R.; Hay, P. J. *J. Chem. Phys.* **1985**, *82*, 284–298.
(71) Andrae, D.; Häußermann, U.; Dolg, M.; Stoll, H.; Preuss, H. *Theor. Chim. Acta* **1990**, *77*, 123–141.
(72) (a) Yamaguchi, K.; Takahara, Y.; Fueno, T. *Appl. Quant. Chem., Proc. Nobel Laureate Symp.*; Reidel: Dordrecht, The Netherlands, 1986; pp 155−184. (b) Noodleman, L.; Norman, J. G. *J. Chem. Phys.* **1979**, *70*, 4903–4906. (c) Noodleman, L. *J. Chem. Phys.* **1981**, *74*, 5737–5743. (d) Noodleman, L.; Case, D. *Adv. Inorg. Chem.* **1992**, *38*, 423–470.
(73) Cances, E.; Mennucci, B.; Tomasi, J. *J. Chem. Phys.* **1997**, *107*, 3032–3041.
(74) Quiñonero, D.; Morokuma, K.; Geletii, Y. V.; Hill, C. L.; Musaev, D. G. *J. Mol. Catal. A: Chem.* **2007**, *262*, 227–235.
(75) Pichon, C.; Mialane, P.; Dolbecq, A.; Marrot, J.; Rivière, E.; Keita, B.; Nadjo, L.; Sécheresse, F. *Inorg. Chem.* **2007**, *46*, 5292–5301.
(76) Drewes, D.; Piepenbrink, M.; Krebs, B. *J. Cluster Sci.* **2006**, *17*, 361–374.
(77) Romo, S.; Fernandez, J. A.; Maestre, J. M.; Keita, B.; Nadjo, L.; de Graaf, C.; Poblet, J. M. *Inorg. Chem.* **2007**, *46*, 4022–4027.
(78) Drewes, D.; Limanski, E. M.; Krebs, B. *Dalton Trans.* **2004**, 2087–2091.
(79) Zueva, E. M.; Chermette, H.; Borshch, S. A. *Inorg. Chem.* **2004**, *43*, 2834–2844.
(80) Botar, B.; Geletii, Y. V.; Kögerler, P.; Musaev, D. G.; Morokuma, K.; Weinstock, I. A.; Hill, C. L. *J. Am. Chem. Soc.* **2006**, *128*, 11268–11277.
(81) Anderson, T. M.; Neiwert, W. A.; Kirk, M. L.; Piccoli, P. M. B.; Schultz, A. J.; Koetzle, T. F.; Musaev, D. G.; Morokuma, K.; Cao, R.; Hill, C. L. *Science* **2004**, *306*, 2074–2077.
(82) Anderson, T. M.; et al. *J. Am. Chem. Soc.* **2005**, *127*, 11948–11949.

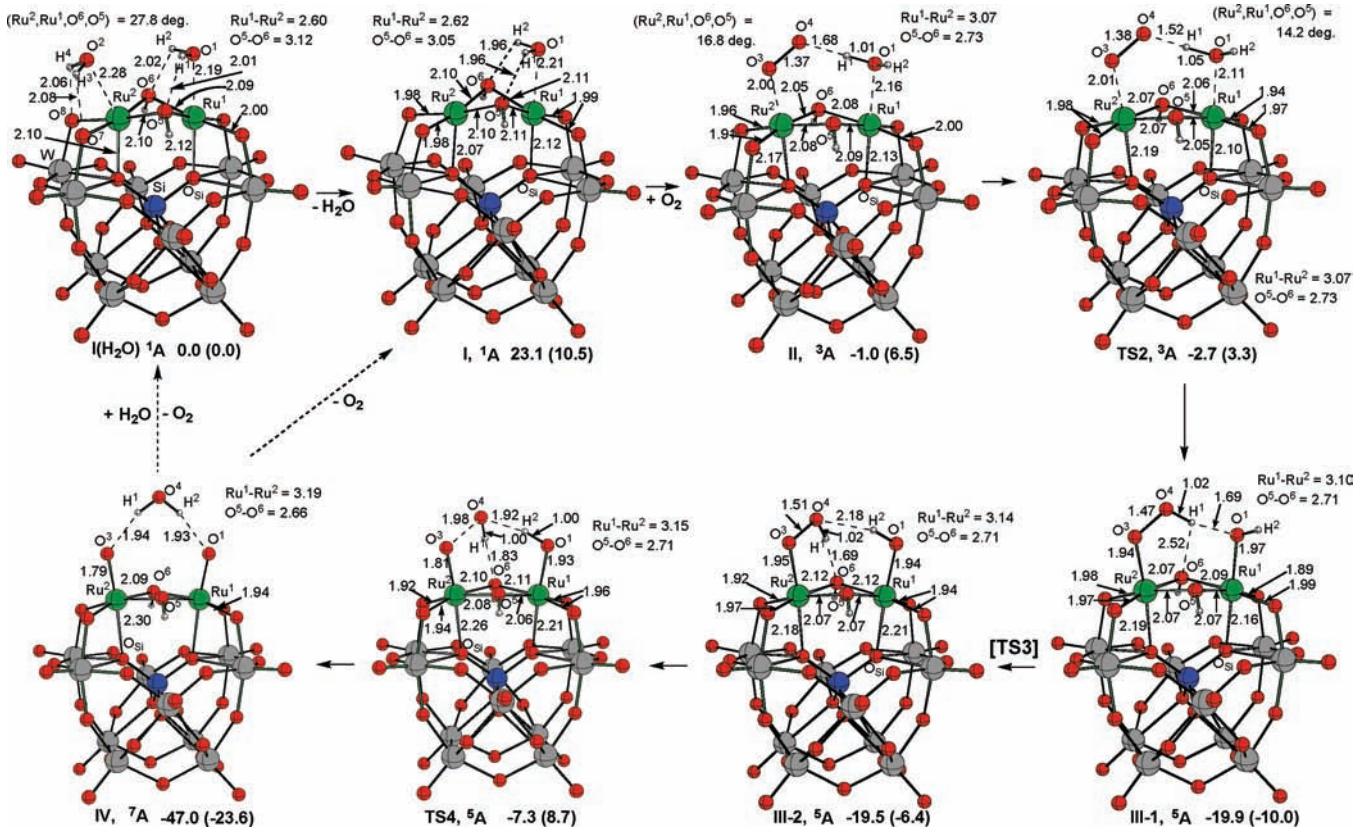

Figure 1. The calculated important geometry parameters (distances in Å, angles in deg) of the reactants, transition states, intermediates, and products of the stepwise pathway of the reaction of $\{\gamma\text{-}[(H_2O)Ru^{III}-(\mu\text{-}OH)_2-Ru^{III}(H_2O)][SiW_{10}O_{36}]\}^{4-}$, **I(H$_2$O)**, with O_2. The presented relative energies ΔE (and $\Delta E + \Delta G_{solv(water)}$ in parentheses) are given in kcal/mol.

such insignificant geometry changes, the calculated **1−(H$_2$O)$_2$** binding energy in **I(H$_2$O)** is found to be large, −43.0 (−26.2) kcal/mol.

It should be noticed that in **I(H$_2$O)** the calculated $Ru-O_{(H_2O)}$ bond distances (2.19 and 2.28 Å) are comparable to those reported by Yang and Baik for $\{(bpy)_2[(H_2O)Ru^{III}-(\mu\text{-}O)-Ru^{III}(OH_2)](bpy)_2\}^{4+}$ (2.252 and 2.250 Å for the triplet staggered and 2.223 and 2.288 Å for the triplet eclipsed configurations).[39] Yet these values are slightly longer than the numbers (2.136 Å (experimental value)[83] and 2.164 Å (calculated value)[60]) found by Meyer and co-workers for the same complex. As expected, geometries of the $[Ru^{III}-(\mu\text{-}OH)_2-Ru^{III}]$ core of **I(H$_2$O)** and $\{Ru^{III}-(\mu\text{-}O)-Ru^{III}\}$ core of the "blue-dimer" are quite different, and the "blue-dimer" can easily rotate around the $\{Ru^{III}-(\mu\text{-}O)-Ru^{III}\}$ axis, while **I(H$_2$O)** cannot.

The next step of the reaction is substitution of one H_2O molecule in **I(H$_2$O)** by a dioxygen molecule to form the intermediate with an $\{(O_2)Ru-(\mu\text{-}OH)_2-Ru(H_2O)\}$ core. As the O_2 molecule comes in, there may exist a complex in which O_2 is bound to the coordinated water molecules but not to the metal centers, analogous to the dioxygen−diruthenium complex $\{(bpy)_2[(H_2O)Ru-(\mu\text{-}O)-Ru(OH_2)](bpy)_2\}^{4+}\cdots O_2$ reported by Yang and Baik.[39] However, we were unable to locate the complex with a $\{Ru(H_2O)-(\mu\text{-}OH)_2-Ru(H_2O)\}\cdots O_2$ motif. Because hydrogen atoms of the coordinated H_2O molecules in **I(H$_2$O)** form quite strong H-bonds with the O-atoms of both OH-bridges and POM framework, they are not available for interaction with the coming O_2 molecule. As seen in Figure 1, ligand environments of Ru^1 and Ru^2 atoms in **I(H$_2$O)** are different, which makes the Ru centers electronically different as well; the calculated Mulliken charges are 0.69e and 0.48e for Ru^1 and Ru^2, respectively. Thus, Ru^2 is more electron-rich and should be more prone to attacks by electrophilic species, that is, O_2 molecule. Therefore, we substitute the H_2O ligand on Ru^2 by O_2.

In general, the water-to-dioxygen substitution reaction may proceed via two different pathways: the stepwise or dissociative pathway and the concerted or associative pathway. The stepwise pathway occurs in two steps: (1) dissociation of water molecule from **I(H$_2$O)** to form $\{\gamma\text{-}[Ru^{III}-(\mu\text{-}OH)_2-Ru^{III}(H_2O)][SiW_{10}O_{36}]\}^{4-}$, **I**, and (2) addition of the O_2 molecule to Ru^2 to form complex $\{\gamma\text{-}[(O_2)Ru^{III}-(\mu\text{-}OH)_2-Ru^{III}(H_2O)][SiW_{10}O_{36}]\}^{4-}$, **II**. In the concerted or associative pathway, substitution of water by O_2 occurs in a single step via a H_2O-to-O_2 substitution transition state [**TS1(H$_2$O)**] and leads to the complex **II(H$_2$O)**, where the substituted water molecule stays in the vicinity of the $\{(O_2)Ru-(\mu\text{-}OH)_2-Ru(H_2O)\}$ core and is H-bonded to it. Let us discuss these two pathways separately.

B. Stepwise or Dissociative Pathway of I(H$_2$O) Oxidation by O$_2$. The first step of the stepwise pathway is the dissociation of one of the water molecules:

$$\mathbf{I(H_2O)} \rightarrow H_2O + \{\gamma\text{-}[Ru^{III}\text{-}(\mu\text{-}OH)_2-Ru^{III}(H_2O)][SiW_{10}O_{36}]\}^{4-}, \mathbf{I}$$

The calculations show that this reaction requires 23.1 (10.5) kcal/mol of energy. Scanning of the potential energy surface of the reverse reaction by choosing the Ru^2-O^2 distance as a

(83) Gilbert, J. A.; Eggleston, D. S.; Murphy, W. R., Jr.; Geselowitz, D. A.; Gersten, S. W.; Hodgson, D. J.; Meyer, T. J. *J. Am. Chem. Soc.* **1985**, *107*, 3855–3864.

Table 1. Calculated Mulliken Atomic Spin Densities (in e), as Well as $\langle S^2 \rangle$ Values

species	**II**, ^{3}A	**TS2**, ^{3}A	**III-1**, ^{5}A	**III-2**, ^{5}A	**TS4**, ^{5}A	**IV(H$_2$O)**, ^{7}A
Ru^1	0.86	1.21	1.44	1.43	1.42	1.64
Ru^2	1.36	0.98	1.26	1.33	1.55	1.64
O^1	0.00	0.00	0.10	0.21	0.25	0.88
O^3	−0.40	−0.47	0.34	0.25	0.63	0.88
O^4	−0.55	−0.46	0.09	0.02	−0.69	0.02
O^5	0.04	0.10	0.08	0.08	0.09	0.07
O^6	0.08	0.09	0.04	0.02	0.05	0.07
O^7	0.26	0.11	0.12	0.12	0.18	0.19
O^8	0.15	0.10	0.11	0.21	0.23	0.19
$\langle S^2 \rangle$	2.84	2.89	6.02	6.02	6.59	12.04

reaction coordinate shows that it occurs with no energy barrier. The ground electronic state of the product complex $\{\gamma$-$[Ru^{III}(\mu\text{-}OH)_2Ru^{III}(H_2O)][SiW_{10}O_{36}]\}^{4-}$, **I**, is found to be a singlet, although we did not explore all of the possible spin states in detail, as this does not make a large difference in the mechanism of the O_2 activation reaction we are studying. As seen in Figure 1, dissociation of a water molecule from **I(H$_2$O)** does not change significantly the geometry of the POM unit of **I(H$_2$O)**. Indeed, in **I**, the Ru^1−Ru^2, Ru^1−O^5/O^6, and Ru^1−O^1 bond distances are elongated by 0.02, 0.02, and 0.02 Å, respectively, and the Ru^2−O_{Si}, O^6−H^2, and O^5−H^1 bond distances are shortened by 0.03, 0.06, and 0.05 Å, respectively, as compared to their values in **I(H$_2$O)**.

At the next stage, O_2 molecule coordinates to **I** to form complex $\{\gamma$-$[(O_2)Ru^{III}(\mu\text{-}OH)_2Ru^{III}(H_2O)][SiW_{10}O_{36}]\}^{4-}$, **II**, with the triplet ground electronic state. O_2 coordination to **I** occurs without a barrier. As seen in Figure 1, the coordination of O_2 to **I** leads to quite drastic geometrical changes. In **II** as compared to **I**, the diamond-like $\{Ru(\mu\text{-}OH)_2Ru\}$ core is distorted significantly; the Ru^1−Ru^2 bond is elongated by 0.45 Å, the O^5−O^6 distance is shortened by 0.32 Å, and the entire $\{Ru(\mu\text{-}OH)_2Ru\}$ core becomes flattened. Also, the Ru−O_{Si} bond distances are elongated, which is especially pronounced for the Ru^2−O_{Si} bond (i.e., for the Ru-center that interacts with O_2 unit). In **II**, the oxygen molecule is coordinated to the Ru^2-atom with one of its O-atoms. The other atom of O_2 is H-bonded to the Ru^1-coordinated water molecule. As seen in Figure 1, the calculated Ru^2−$O^3(O_2)$ and O^4−H^1 (from the water) bond distances are 2.00 and 1.68 Å, respectively. As a result of these interactions, the O−O bond is elongated by 0.16 Å in **II** as compared to that in the free dioxygen molecule. The computed O−O bond distance of 1.37 Å in **II** implies superoxo character of the coordinated O_2-unit; the calculations performed at the same level of theory gave 1.42 and 1.68 Å for O−O bond distances in free O_2^- and O_2^{2-} species, which is in reasonable agreement with the experimental value of 1.35 Å for O_2^-[84] and calculated values of 1.64 Å (with the SD-CI approach) and 1.67 Å (with the SAC-CI approach)[85] for O_2^{2-}, respectively.

The superoxide character of the O_2-unit in **II** is also supported by the results of spin density analysis; in **II**, O_2 bears about one unpaired β-spin (0.40e on the O^3-atom and 0.55e on O^4) (see Table 1).

Calculations show noticeable charge transfer from Ru^1 and Ru^2 to O^1 and O^3, respectively (see the Supporting Information). The Ru^2 and Ru^1 atoms of **II** bear 1.36e and 0.86e α-spin densities, respectively; that is, about 0.73e α-spin density is delocalized over other atoms of the compound. Thus, formally, the Ru^2 and Ru^1 atoms in **II** could be considered as having oxidation states of +4 (with two spins) and +3 (with one spin), respectively; that is, upon substitution of water by O_2 the Ru^2-center of **I** is oxidized by one electron. However, it should be noted that the calculated $\langle S^2 \rangle$ value for triplet **II** is 2.84, which is significantly larger than its ideal value of 2.0. This indicates some mixing in the wave function of the triplet **II** from those of high-spin states (for example, quintet state). In fact, the calculated quintet state of **II** has a very similar geometry and lies only 3.6 kcal/mol higher in energy than its ground triplet state; in the quintet state, the superoxo unit bears about 1.0e α-spin density (rather than β-spin density in the triplet).

Comparison of the calculated geometries and electronic structure of **II** with those for the superoxo−aqua complex of the "blue-dimer", $\{(bpy)_2[(OO)Ru(\mu\text{-}O)Ru(OH_2)](bpy)_2\}^{4+}$ reported by Yang and Baik,[39] shows the following important differences: (i) Ru−OO and $Ru-OH_2$ bond distances differ only slightly between these complexes; however, the superoxo O−O and $O_{(O-O)}$−$H_{(H_2O)}$ bond distances in the "blue-dimer" are ca. 0.07 Å shorter than in **II**; and (ii) **II** favors the triplet ground state with ferromagnetically coupled Ru^1(III) and Ru^2(IV) atoms and antiferromagnetically coupled Ru^2(IV) and O−O moiety. However, the ground state of the "blue-dimer" intermediate is reported to be the quintet state with Ru centers and O−O unit all ferromagnetically coupled. The most viable explanations of why **II** and $\{(bpy)_2[(OO)Ru(\mu\text{-}O)Ru(OH_2)](bpy)_2\}^{4+}$ have different ground electronic states lie in: (a) structural flexibility of the Ru−O−Ru unit of the "blue-dimer" as compared to that of the $\{Ru(OH)_2Ru\}$ unit in **II**; (b) the ability of the O bridge to undergo notable variations of its spin density as compared to the μ-OH bridges of POM system; and (c) the difference in electronic nature of bpy (which is a strong π-acceptor) and the POM (which is a π-acceptor and σ-donor).

Indeed, as seen in Table 1, the bridging OH groups of **II** have only insignificant amount of unpaired spins (0.04 and 0.08e), while Yang and Baik[39] have reported 0.50e β-spin on the bridging O^1-center of $\{Ru(OO)(\mu\text{-}O^1)Ru(H_2O)\}$. The overall H_2O-to-O_2 substitution reaction, that is, **I(H$_2$O)** → **I** → **II** (dissociation of water molecule and coordination of O_2), is found to be slightly exothermic (by 1.0 kcal/mol) in the gas phase, but (6.5 kcal/mol) endothermic in water.

From complex **II** the reaction proceeds via the H-atom (H^1) transfer transition state **TS2** to give the hydroperoxo−hydroxo complex $\{\gamma$-$[(OOH)Ru(\mu\text{-}OH)_2Ru(OH)][SiW_{10}O_{36}]\}^{4-}$, **III**, which could have several isomers, and below we discuss only two, the most stable of them referred to as **III-1** and **III-2**. Comparison of the important geometry parameters of **TS2** with those for **II** shows that in **TS2** (a) the dissociating O^1−H^1 bond is elongated by only 0.04 Å, (b) the forming Ru^1−O^1 and O^4−H^1 bond distances are shortened by 0.05 and 0.16 Å, respectively, (c) the O^3−O^4 and Ru^2−O^3 bond distances are elongated by only 0.01 Å, and (d) Ru^1−O_{Si} and Ru^2−O_{Si} bond distances are shortened by 0.03 Å and elongated by 0.02 Å, respectively. Thus, geometry changes upon going from the complex **II** to the transition state **TS2** are not significant; therefore, **TS2** should be considered as an early transition state. This conclusion is consistent with the calculated spin densities (see Table 1) and the energy barrier at **TS2**. Indeed, in **TS2** the atoms of the superoxo unit O^3−O^4 possess spin densities, 0.47e on the O^3 and 0.46e on the O^4, which are close to those in **II**. The Mulliken charge on the transferred H^1 atom is +0.44e. The energy of

(84) Linstrom, P. J.; Mallard, W. G. NIST Chemistry WebBook, NIST Standard Reference Database Number 69, March 2003, National Institute of Standards and Technology, Gaithersburg MD, 20899. Available from: http://webbook.nist.gov.
(85) Nakatsuji, H.; Nakai, H. *Chem. Phys. Lett.* **1992**, *197*, 339–345.

transition state **TS2** relative to **II** is slightly negative, −1.7 (−3.2) kcal/mol (at the B3LYP/SDD level of theory), although it is a real transition state and has a relative energy of +2.4 (+1.5) kcal/mol at the B3LYP/[Lanl2dz + d(Si)] level used for geometry optimization.

Overcoming of this insignificant barrier leads to the formation of the hydroperoxo−hydroxo intermediate **III-1**. Our extensive studies of several lower-lying electronic state of this complex clearly show the quintet ground state, while its antiferromagnetically coupled open-shell singlet state lies 7.1 kcal/mol higher at the B3LYP/[Lanl2dz + d(Si)] level used for geometry optimization. As seen in Figure 1, in **III-1**, the O^3-O^4 bond distance is elongated by 0.09 Å and the formed Ru^2-O^3 and Ru^1-O^1 bond distances are shortened by 0.06 and 0.19 Å, relative to **II**. The formed O^4-H^1 bond becomes 1.02 Å long, with the H^1 hydrogen bonded to the terminal O^1H^2-ligand. The calculated Ru^1-O^1 and Ru^2-O^3 bond distances show the existence of the covalent bond between the Ru-centers and OOH and OH groups, respectively. During the reaction **II** → **TS2** → **III-1**, the geometry of the $\{Ru-(\mu\text{-}OH)_2-Ru\}$ core remains almost unchanged, and $Ru-O_{Si}$ bond distances are only increased slightly, by 0.02 and 0.03 Å. However, the Mulliken charges and spin densities change significantly upon going from **II** to **III-1**; the total spin density on the O^3-O^4 moiety changes from −0.95e (β-spin) to 0.43e (α-spin), while on the Ru^1 and Ru^2 atoms it increases from 2.2e to 2.7e (α-spins). Thus, about 0.87e spin is distributed over the POM framework atoms. Both Ru^1 and Ru^2 can be considered formally as Ru^{IV} centers in the complex **III-1**. Thus, the proton transfer from the coordinated water molecule to the superoxo unit has completed 1e-oxidation of each Ru-center of Ru_2-substituted-γ-Keggin polyoxotungstate. As seen in Figure 1, formation of the hydroperoxo−hydroxo species **III-1** is exothermic by 18.9 (16.5) kcal/mol, calculated relative to the complex **II**.

For the reaction to proceed further, the intermediate **III-1** has to rearrange into an isomer **III-2**, where the bridging O^6H group is H-bonded to the OOH group. Calculations show that **III-2** also has the quintet ground state and is only 0.4 (3.6) kcal/mol higher in energy than the isomer **III-1**, where the coordinated OOH group is H-bonded to bridging and terminal OH groups simultaneously. During the **III-1** → **III-2** rearrangement, the O^1H^2 group is rotated around the Ru^1-O^1. This rearrangement is expected to proceed via a small rotational barrier. However, we were not able to locate the transition state (**TS3**) associated with this barrier. Comparison of the calculated geometries of **III-1** and **III-2** shows noticeable differences; in **III-2**, the Ru^1-Ru^2, O^3-O^4, Ru^1-O^6, and Ru^2-O^6 bond distances are longer by 0.04, 0.04, 0.03, and 0.05 Å, respectively, but the H^1-O^6, Ru^1-O^1, and Ru^2-O^3 bond distances are shorter by 0.83, 0.03, and 0.01 Å, respectively, than in **III-1**. In **III-2**, the H^2-O^4 distance is calculated to be 2.18 Å.

From the intermediate **III-2**, the reaction proceeds via the next 2e-oxidation process, that is, the formation of water, $O^4H^1H^2$, and the complex $\{\gamma\text{-}[(O)Ru-(\mu\text{-}OH)_2-Ru(O)](H_2O)[SiW_{10}O_{36}]\}^{4-}$, **IV**, with an $\{ORu-(\mu\text{-}OH)_2-RuO)\}$ core. Reaction **III-2** → **IV** proceeds with a 12.2 (15.1) kcal/mol barrier (calculated from the intermediate **III-2**) at the transition state **TS4**, which also has a quintet ground state, as the prereaction complex **III-2**. Interestingly, the comparison of the calculated bond distances of O^3-O^4 = 1.98 Å, O^4-H^2 = 1.92 Å, H^1-O^6 = 1.83 Å, and Ru^2-O^3 = 1.81 Å, for **TS4**, with their values (1.51, 2.18, 1.69, and 1.95 Å, respectively) in the prereaction complex **III-2**, shows that in **TS4** the O^3-O^4, O^1-H^2, and H^1-O^6 bonds are dissociated, and the Ru^2-O^3 and H^2-O^4 bonds are formed in a concerted fashion. Because the O^3-O^4 bond elongation is much larger (0.47 Å) than that of the O^1-H^2 bond (0.01 Å), one may describe **TS4** as the OH-transfer transition state rather than proton transfer one. This is in good agreement with the difference in the peroxo O−O and RO−H bond strengths (ca. 50.3 kcal/mol for the O−O bond in HOOH and ca. 118.8 kcal/mol for the HO−H bond).[86] One also should note that the total charge of the moving OH group is calculated to be only −0.06e. Spin density analysis shows that in the ground quintet state of **TS4** the O^3-O^4 bond acquires significant biradical character (see Table 1); oxygen atoms, originated from the O_2, bear large fractions of unpaired spin density with opposite signs (0.63e at O^3 and −0.69e at O^4), implying the O−O bond breaking at the transition state. The $\{Ru-(\mu\text{-}OH)_2-Ru\}$ core is more flattened in **TS4**, in comparison with **III-2**, although the Ru^1-Ru^2, Ru^1-O^5, and Ru^2-O^6 bond distances are changed only slightly. In the product **IV**, the Ru^1-Ru^2 bond distance is elongated by 0.04 Å, while the O^5-O^6 bond distance is shortened by 0.05 Å in comparison with the reactant **III-2** structure. Yet the most drastic changes occur in Ru^1-O^1 and Ru^2-O^3 bond distances; they are shortened by 0.15 (0.16) Å, which indicates the formation of RuO unit with multiple ruthenium−oxygen bond character. The calculated geometry of **TS4** is closer to that of the reactant **III-2**; thus **TS4** is an early transition state, as expected for an exothermic reaction. The **III-2** → **IV** transformation is calculated to be exothermic by 27.5 (17.2) kcal/mol.

Resulting complex **IV** has a septet ground electronic state, where the formed H_2O^4 molecule is H-bonded to the Ru═O units. The spin density analysis (see Table 1) demonstrates a key electronic feature of **IV**. Indeed, the Ru centers of **IV** bear spin density of 1.64e each, similar to 1.42e and 1.55e at the transition state **TS4**. Its O^1 and O^3 centers (oxo oxygens) have 0.88e unpaired spins each, which are also close to 0.63e and −0.69e reported for the O^3 and O^4 centers (oxygen atoms of the breaking O^3-O^4H bond) of the transition state **TS4**. However, in **IV** all unpaired spins are α-spins, while in **TS4** one of the O-centers (O^4) has a β-spin. So, the transfer of H^2-center from $Ru^1-O^1H^2$ to O^4H^1, after the **TS4**, is accompanied by 0.71e α-spin transfer to the O^4-center. As a result, the O^1-center of Ru^1-O^1 acquires a strong radical character with almost one (0.88 e) α-spin, while the O^4-center of the formed H_2O^4 unit becomes a center with almost no unpaired spin. Thus, the final complex **IV** should be formulated as a species with the $Ru^{IV}-O^{\bullet}$ units, rather than a species having the Ru^{V}═O groups. Similar radicaloid character of the Ru═O-fragments of $\{(bpy)_2[ORu-(\mu\text{-}O)-RuO](bpy)_2\}^{4+}$ intermediate was reported by Yang and Baik; the authors have shown that oxo oxygens of Ru═O groups of the $\{Ru(O)-(\mu\text{-}O)-Ru(O)\}$ core are antiferromagnetically coupled with 0.78e and −0.78e spins, respectively.[39] Furthermore, the $\{(bpy)_2[ORu-(\mu\text{-}O)-RuO](bpy)_2\}^{4+}$ intermediate was reported to have the open shell singlet ground state, whereas intermediate **IV** has a septet ground state. The results presented above clearly show that the reaction **III-2** → **TS4** → **IV** starts from the quintet complex **III-2** with two Ru^{IV} centers, proceeds via the quintet **TS4**, where two O-centers acquire antiferromagnetically coupled α and β-spins, and leads to the complex **IV** by α-to-β-spin flip on O^2 and spin transfer from O^4-center to O^1. As a result, the final product has a septet ground electronic state with the $Ru^{IV}-O^{\bullet}$ radicaloid character.

(86) *CRC Handbook of Chemistry and Physics*, 86th ed.; Lide, D. R., Ed.; CRC Press: Boca Raton, FL, 2005.

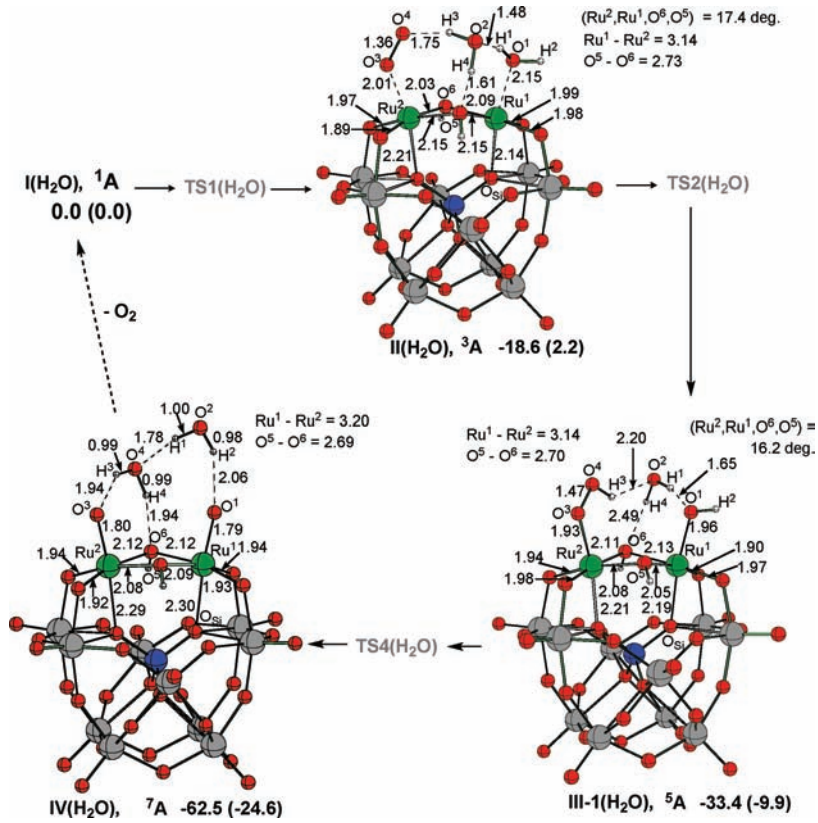

Figure 2. The calculated important geometry parameters (distances in Å, angles in deg) of the reactants, transition states, intermediates, and products of the concerted pathway of the reaction of $\{\gamma\text{-}[(H_2O)Ru^{III}(\mu\text{-}OH)_2Ru^{III}(H_2O)][SiW_{10}O_{36}]\}^{4-}$, **I(H$_2$O)**, with O_2. The presented relative energies ΔE (and $\Delta E + \Delta G_{solv(water)}$ in parentheses) are given in kcal/mol.

One should note that the antiferromagnetically coupled broken-symmetry electronic state of **IV** is only 3.1 kcal/mol higher in energy at the B3LYP/[Lanl2dz + d(Si)] level.

C. Concerted or Associative Pathway of I(H$_2$O) Oxidation by O$_2$ Molecule. As mentioned above, the concerted or associative pathway of the reaction under the study also starts from the singlet **I(H$_2$O)** complex, as a stepwise pathway, but, as shown in Figure 2, proceeds via the concerted water-to-dioxygen substitution transition state, **TS1(H$_2$O)**, and leads to the triplet complex $\{\gamma\text{-}[(O_2)Ru^{III}(\mu\text{-}OH)_2Ru^{III}(H_2O)](H_2O)[SiW_{10}O_{36}]\}^{4-}$, **II(H$_2$O)**. In **II(H$_2$O)**, the substituted water molecule is located in the vicinity of the $\{Ru(O_2)(\mu\text{-}OH)_2\text{-}Ru(H_2O)\}$ core and H-bonded to it. Despite substantial efforts, we were not able to optimize the transition state **TS1(H$_2$O)**. This reaction involves complicated ligand reorganizations and might well take place with a low barrier. Although the upper limit of the barrier is the energy (23.1 (10.5) kcal/mol) required for water dissociation from **I** reported above, it is not likely that such complete water dissociation is needed for this concerted substitution process. Thus, this step of the concerted pathway is likely to take place easier than that of the stepwise pathway discussed above.

As seen in Figure 2, after substitution of the coordinated water molecule, $O^2H^3H^4$, by dioxygen, it forms an H-bonding network between the coordinated O_2, another coordinated water molecule, and one of the OH-bridges of **II(H$_2$O)**: the calculated O^4-H^3, O^5-H^4, and O^2-H^1 distances are 1.75, 1.61, and 1.48 Å, respectively. The comparison of other geometry parameters of **II(H$_2$O)** with those for **II** shows that the presence of water molecule in the vicinity of the $\{(O_2)Ru(OH)_2Ru(H_2O)\}$ core does not significantly change the Ru^1-O^1, Ru^2-O^3, and O^3-O^4 bond distances. However, Ru^1-Ru^2, Ru^1-O^5, and Ru^2-O^5 bond distances in **II(H$_2$O)** are elongated by 0.07, 0.06, and 0.07 Å, respectively. Also, $Ru-O_{Si}$ bond distances are slightly longer in **II(H$_2$O)** than **II**. These geometry changes are consistent with the calculated exothermicity of the reaction **II** + **H$_2$O** → **II(H$_2$O)** of 17.6 (4.3) kcal/mol.

At the next stage, the resulting complex **II(H$_2$O)** rearranges into a quintet hydroperoxo−hydroxo intermediate $\{\gamma\text{-}[(OO\text{-}H)Ru(\mu\text{-}OH)_2Ru(OH)](H_2O)[SiW_{10}O_{36}]\}^{4-}$, **III-1(H$_2$O)**, via the proton-transfer transition state **TS2(H$_2$O)** (see Scheme 1). All of our attempts to locate this transition state (where H^3 and H^1 will transfer to O^4 and O^2, respectively, in concerted ways) connecting the reactant **II(H$_2$O)** with the product **III-1(H$_2$O)** have failed: all calculations converge either to the reactant or to the product. As we have demonstrated above for the stepwise pathway, such proton-transfer processes are extremely facile and occur with little (or no) energy barrier. On the basis of (a) our numerous attempts, (b) mentioned findings for the stepwise pathway, as well as (c) the calculated bond distances in the prereaction complex **II(H$_2$O)** ($O^4-H^3 = 1.75$ Å, $O^5-H^4 = 1.61$ Å, and $O^2-H^1 = 1.48$ Å), we conclude that the proton transfers in **II(H$_2$O)** to form **III-1(H$_2$O)** would occur also with a small (or no) energy barrier, although we were not able to find the exact transition state associated with it.

Comparison of the calculated geometries of **II(H$_2$O)** with those of the hydroperoxo−hydroxo **III-1(H$_2$O)** species shows several notable differences: in **III-1(H$_2$O)**, the O^3-O^4 bond distance is elongated by 0.11 Å, while the Ru^2-O^3 and Ru^1-O^1 bond distances are shorter by 0.08 and 0.19 Å, respectively, than in **II(H$_2$O)**. In **III-1(H$_2$O)**, the coordinated water molecule changes its orientation relative to the $\{Ru-(\mu\text{-}OH)_2-Ru\}$ core, and hydrogen bonds between the water molecule and the

Scheme 1. Schematic Presentation of the Possible Intermediates and Transition States of the Associative Pathway of the Reaction $\{\gamma\text{-}[(H_2O)Ru^{III}(\mu\text{-}OH)_2Ru^{III}(H_2O)][SiW_{10}O_{36}]\}^{4-}$, **I(H$_2$O)**, with O_2[a]

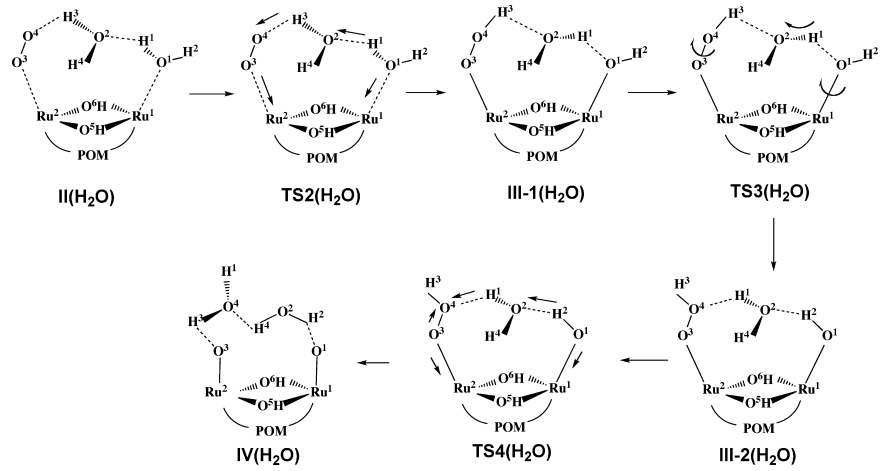

[a] Arrows show the possible reaction coordinates.

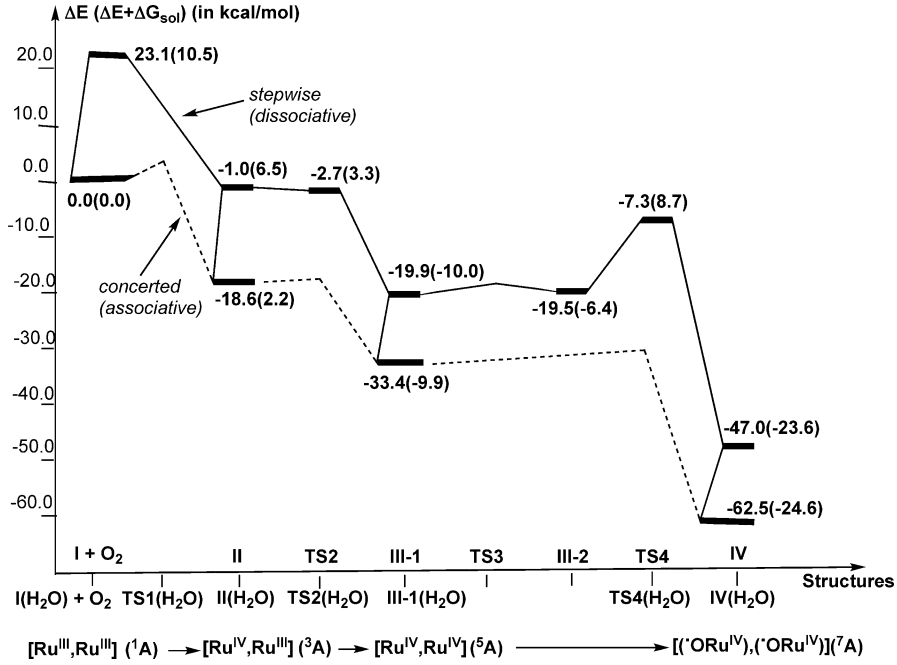

Figure 3. Schematic presentation of the potential energy surface of the stepwise and concerted pathways of the reaction of $\{\gamma\text{-}[(H_2O)Ru^{III}(\mu\text{-}OH)_2Ru^{III}(H_2O)][SiW_{10}O_{36}]\}^{4-}$, **I(H$_2$O)**, with O_2. The presented relative energies ΔE (and $\Delta E + \Delta G_{solv(water)}$ in parentheses) are given in kcal/mol.

$\{Ru(OOH)-(\mu\text{-}OH)_2-Ru(OH)\}$ moiety are elongated as compared to those in the prereaction complex **II(H$_2$O)**. Also, the geometry of the $\{Ru-(\mu\text{-}OH)_2-Ru\}$ core changes considerably: the O^5-O^6, Ru^1-O^5, and Ru^2-O^5 bond distances are shrunk by 0.03, 0.1, and 0.07 Å, respectively, while the Ru^2-O^6 and Ru^1-O^6 bond distances are elongated by 0.08 and 0.04 Å, correspondingly. The rearrangement of the triplet **II(H$_2$O)** complex into the quintet hydroperoxo−hydroxo **III-1(H$_2$O)** compound is found to be exothermic by 14.8 (12.1) kcal/mol.

As seen in Scheme 1, starting from the **III-1(H$_2$O)** complex, the reaction should proceed along the **III-2(H$_2$O)** formation pathway, that is, **III-1(H$_2$O)** → **III-2(H$_2$O)** isomerization. This isomerization process is expected to proceed via the **TS3(H$_2$O)** transition state, which is associated with rotations of O^1H^2, $H^4O^2H^1$, and $O^3O^4H^3$ fragments. This step of the reaction is also expected to occur with a small barrier and be almost thermoneutral. Therefore, here we did not calculate the structure **III-2(H$_2$O)** and transition state **TS3(H$_2$O)**. The resulting complex **III-2(H$_2$O)** should rearrange to the complex $(H_2O)_2\cdots\{\gamma\text{-}[(O)Ru-(\mu\text{-}OH)_2-Ru(O)][SiW_{10}O_{36}]\}^{4-}$, **IV(H$_2$O)**, via the multicentered proton-transfer transition state, **TS4(H$_2$O)**. Calculations show that product **IV(H$_2$O)** with an $(H_2O)_2\cdots\{(O)Ru-(\mu\text{-}OH)_2-Ru(O)\}$ core has a septet ground electronic state.

The structure of the product species **IV(H$_2$O)** with the $\{Ru(O)-(\mu\text{-}OH)_2-Ru(O)\}\cdots(H_2O)_2$ core is given in Figure 2. As seen from the figure, again the H-network is formed (a) between the oxygen atoms of the Ru=O units and coordinated water molecules, (b) between two coordinated water molecules, and (c) between the coordinated water molecule and one of the OH-bridges of **IV(H$_2$O)**: the calculated O^3-H^3, O^6-H^4, O^4-H^1, and O^1-H^2 distances are 1.94, 1.94, 1.78, and 2.06 Å, respectively. In the product **IV(H$_2$O)**, the Ru^1-Ru^2 bond distance is elongated by 0.06 Å, and the O^5-O^6 distance is shrunk by a mere 0.01 Å in comparison with the reactant **III-**

1(H$_2$O) structure. The Ru^1−O^6 and Ru^2−O^6 bond distances becomes slightly shortened and elongated, respectively, by a mere 0.01 Å, and the Ru^1−O^5 bond distance is elongated by 0.04 Å. Yet the most drastic changes occur in the Ru^1−O^1 and Ru^2−O^3 bond distances: they are shrunk by 0.17 and 0.13 Å, respectively, indicating the formation of Ru═O double bonds; also, the Ru^1−O$_{Si}$ and Ru^2−O$_{Si}$ bond distances are noticeably elongated, by 0.11 and 0.08 Å, respectively. The Ru^1−O^1 and Ru^2−O^3 and also Ru−O$_{Si}$ bond distances in **IV(H$_2$O)** are very similar to those in the **IV** species. The **III-1(H$_2$O)** → **IV(H$_2$O)** transformation is calculated to be exothermic by 29.1 (14.7) kcal/mol.

We should mention here that the associative and dissociative pathways are also connected by the association/dissociation of a water molecule at the intermediates **II**, **III**, and **IV**.

D. Discussion. The overall potential energy surface of the reaction of **I(H$_2$O)** with O_2 molecule is presented in Figure 3. As seen from the figure, the overall reaction is highly exothermic. The stepwise or dissociative pathway of this reaction, that is, **I(H$_2$O)**(^{1}A) + O_2 → **I** → **II**(^{3}A) + H_2O → **TS2**(^{3}A) + H_2O → **III-1**(^{5}A) + H_2O → **III-2**(^{5}A) + H_2O → **TS4** → **IV**(^{7}A) + H_2O, is found to be 47.0 (23.6) kcal/mol exothermic and proceeds with a 23.1 (10.5) kcal/mol energy required for dissociation of one of the water molecules from **I(H$_2$O)**; that is, at the first step of the reaction, **I(H$_2$O)**(^{1}A) + O_2 → **I** → **II**(^{3}A) + H_2O. However, the concerted or associative mechanism of this reaction, **I(H$_2$O)**(^{1}A) + O_2 → [**TS1(H$_2$O)**] → **II(H$_2$O)**(^{3}A) → [**TS2(H$_2$O)**] → **III-1(H$_2$O)**(^{5}A) → [**TS4(H$_2$O)**] → **IV(H$_2$O)**(^{7}A), seems kinetically and thermodynamically more favorable. Although we could find none of the transition states, most likely because of low barriers, it is more exothermic (by 15.5 (1.0) kcal/mol).

The entire reaction **I(H$_2$O)** + O_2 is a 4-electron oxidation process. The first 1e-oxidation (of the Ru^2-center) occurs after the H_2O → O_2 substitution, that is, in the step **I**(^{1}A) → **II**(^{3}A) and **I(H$_2$O)**(^{1}A) → **II(H$_2$O)**(^{3}A), for dissociative and associative pathways, respectively. The second 1e-oxidation (of the Ru^1-center) is completed upon the proton-coupled-electron (hydrogen atom) transfer from the Ru^1-coordinated water molecule to the Ru^2-coordinated superoxide to form a hydroperoxo−hydroxo intermediate, that is, in the steps **II**(^{3}A) → **III-1**(^{5}A) and **II(H$_2$O)**(^{3}A) → **III-1(H$_2$O)**(^{5}A), for dissociative and associative pathways, respectively. The final 2e-oxidation occurs upon the proton transfer from the Ru^1-coordinated terminal OH-ligand to the Ru^2-coordinated OOH fragment to form the water molecule and the complex with two Ru═O units, that is, in steps **III-2**(^{5}A) → **IV**(^{7}A) and **III-1(H$_2$O)**(^{5}A) → **IV(H$_2$O)**(^{7}A) on the stepwise and concerted pathways, respectively. Resulting complexes **IV** and **IV(H$_2$O)** have a septet ground electronic state with the radical terminal oxo groups and should be formulated as species with the Ru^{IV}═O$^•$ units, rather than species having the Ru^V═O groups. Similar radicaloid character of the Ru═O-fragments of $\{(bpy)_2[ORu-(\mu\text{-}O)-RuO](bpy)_2\}^{4+}$ intermediate of the "blue-dimer" was reported by Yang and Baik.[39]

Thus, the presented results show (Figure 3) that oxidation of **I(H$_2$O)** by O_2 molecule is a kinetically and thermodynamically facile process and can occur at room temperature. The product of this reaction is the complex **IV** or **IV(H$_2$O)** with an $\{(^•O)Ru-(\mu\text{-}OH)_2-Ru(O^•)\}$ core. Consequently, the "reverse" reaction, that is, O_2 formation from **IV** or **IV(H$_2$O)**, is highly [by 47.0(23.6) and 62.5(24.6) kcal/mol for stepwise and concerted pathways, respectively] endothermic and cannot occur. This conclusion is drastically different from that reported for the "blue-dimer" $\{(bpy)_2[ORu-(\mu\text{-}O)-RuO](bpy)_2\}^{4+}$ intermediate, which has been established to oxidize incoming water molecule to produce O_2.[2,5,29−35,39,41,60−62]

It is of core importance to elucidate the reasons for the dramatic reactivity difference of $[(bpy)_2Ru(O^•)-(\mu\text{-}O)-Ru(O^•)(bpy)_2]^{4+}$ and $\{\gamma\text{-}[(^•O)Ru-(\mu\text{-}OH)_2-Ru(O^•)](H_2O)[SiW_{10}O_{36}]\}^{4-}$, **IV**. For this purpose, we have recalculated the structures and energies of the $[(bpy)_2Ru-(\mu\text{-}O)-Ru(bpy)_2]^{4+}$, $[(bpy)_2Ru(O^•)-(\mu\text{-}O)-Ru(O^•)(bpy)_2]^{4+}$, and $[(bpy)_2Ru(H_2O)-(\mu\text{-}O)-Ru(H_2O)(bpy)_2]^{4+}$ complexes at the B3LYP/lanl2dz level of theory in their ground electronic states. These structures and their important geometry parameters are given in Figure 4.

For easy comparison, we also present in Figure 4 the results for $\{\gamma\text{-}[Ru-(\mu\text{-}OH)_2-Ru][SiW_{10}O_{36}]\}^{4-}$, **1**, and **IV** calculated at the B3LYP/[Lanl2dz + d(Si)] level of theory.

At first, these calculations show that the water oxidation by the "blue-dimer", that is, the reaction

$$\{(bpy)_2[Ru(O^•)-(\mu\text{-}O)-Ru(O^•)](bpy)_2\}^{4+} + 2H_2O \rightarrow \{(bpy)_2[(H_2O)Ru-(\mu\text{-}O)-Ru(H_2O)](bpy)_2\}^{4+} + O_2 \quad (1)$$

is highly, 43.2 kcal/mol, exothermic, while the water oxidation by **IV**, that is, the reaction

$$\{\gamma\text{-}[(^•O)Ru-(\mu\text{-}OH)_2-Ru(O^•)](H_2O)[SiW_{10}O_{36}]\}^{4-} + H_2O \rightarrow \{\gamma\text{-}[(H_2O)Ru-(\mu\text{-}OH)_2-Ru(H_2O)][SiW_{10}O_{36}]\}^{4-} + O_2 \quad (2)$$

is endothermic by 15.1 kcal/mol (here, we report only gas-phase ΔE values of these reactions calculated at the same level of theory). One of the reasons for such a large (by 58.3 kcal/mol) difference in the calculated thermodynamics of these reactions could be the energies of the formed Ru−H_2O bonds in the product complexes. However, our calculations show that, in fact, the Ru−H_2O bond energies are very similar in the Ru_2−POM (structure **I(H$_2$O)**) and in the "blue-dimer": the energies of the reactions

$$\{\gamma\text{-}[(H_2O)R-(\mu\text{-}OH)_2-Ru(H_2O)][SiW_{10}O_{36}]\}^{4-} \rightarrow \{\gamma\text{-}[Ru-(\mu\text{-}OH)_2-Ru][SiW_{10}O_{36}]\}^{4-} + 2H_2O$$

and

$$\{(bpy)_2[(H_2O)Ru-(\mu\text{-}O)-Ru(H_2O)](bpy)_2\}^{4+} \rightarrow \{(bpy)_2[Ru-(\mu\text{-}O)-Ru](bpy)_2\}^{4+} + 2H_2O$$

are calculated to be 55.3 and 64.7 kcal/mol, respectively. Thus, the strength of the formed Ru−H_2O bonds is not a major reason for the observed large difference in thermodynamics between reactions 1 and 2. Consequently, the reason of the calculated difference should be the energies of the reactions

$$\{\gamma\text{-}[(^•O)Ru-(\mu\text{-}OH)_2-Ru(O^•)][SiW_{10}O_{36}]\}^{4-} \rightarrow \{\gamma\text{-}[Ru-(\mu\text{-}OH)_2-Ru][SiW_{10}O_{36}]\}^{4-} + O_2 \quad (3)$$

and

$$\{(bpy)_2[(O^•)Ru-(\mu\text{-}O)-Ru(O^•)](bpy)_2\}^{4+} \rightarrow \{(bpy)_2[Ru-(\mu\text{-}O)-Ru](bpy)_2\}^{4+} + O_2 \quad (4)$$

which are calculated to be 70.4 and 21.5 kcal/mol endothermic, respectively.

The calculated large endothermicity of reaction 3 for Ru_2−POM as compared to that of reaction 4 for the "blue-dimer" could be a result of several factors including the Ru═O and Ru−L [where L = $(SiW_{10}O_{36})^{4-}$ and bpy] bond strengths,

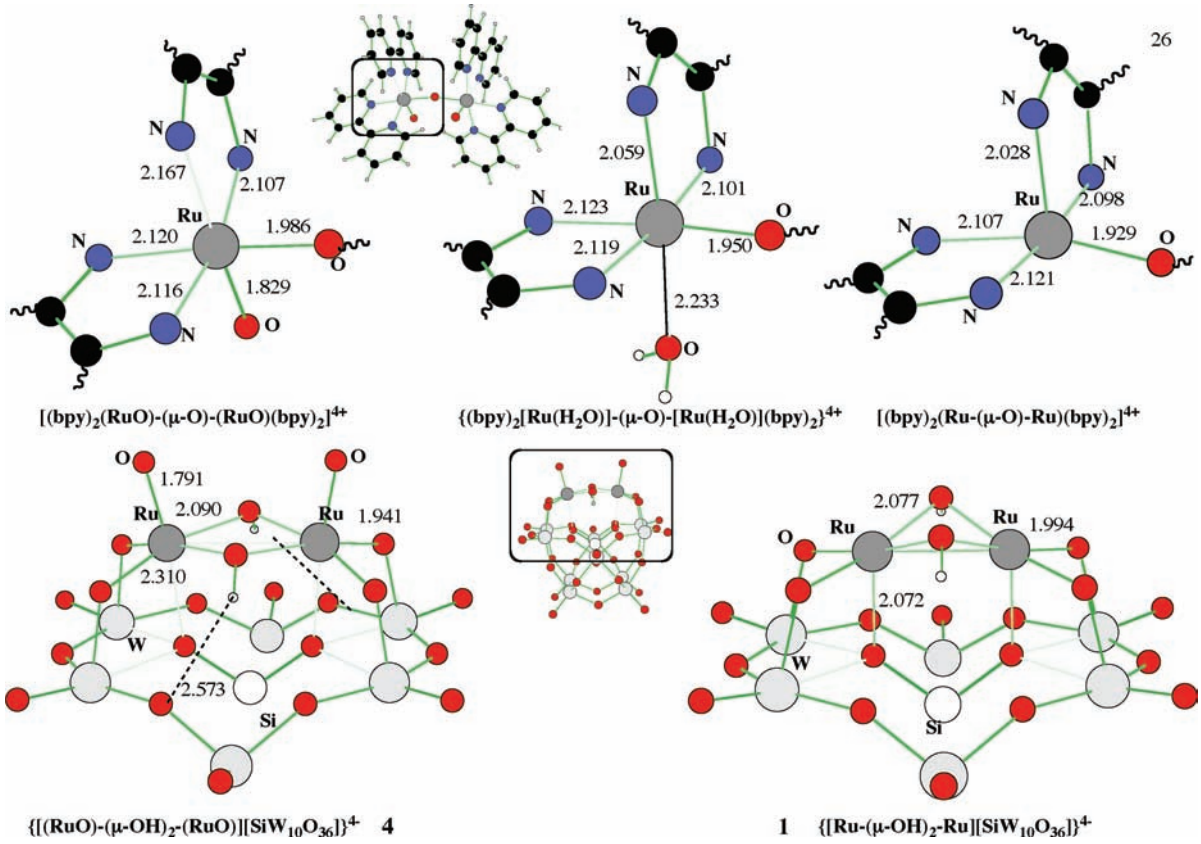

Figure 4. The important geometry parameters (distances in Å, angles in deg) of the complexes $[(bpy)_2Ru(O^{\bullet})-(\mu-O)-Ru(O^{\bullet})(bpy)_2]^{4+}$, $[(bpy)_2Ru(H_2O)-(\mu-O)-Ru(H_2O)(bpy)_2]^{4+}$, and $[(bpy)_2Ru-(\mu-O)-Ru(bpy)_2]^{4+}$, as well as $\{\gamma-[Ru^{III}-(\mu-OH)_2-Ru^{III}][SiW_{10}O_{36}]\}^{4-}$, **1**, and $\{\gamma-[(^{\bullet}O)Ru-(\mu-OH)_2-Ru(O^{\bullet})]-[SiW_{10}O_{36}]\}^{4-}$, **IV**. For the sake of simplicity, we show only the important portions of these structures.

and deformation geometries defined by the L ligands as well as of $\{Ru-(\mu-OH)_2-Ru\}$ and $\{Ru-(\mu-O)-Ru\}$ cores. These parameters all relate to a key experimental variable associated with O_2 activation and H_2O oxidation, the ground-state reduction potentials. Unfortunately, one cannot directly (and accurately) estimate the Ru=O and Ru−L bond strengths in $\{(bpy)_2[(O^{\bullet})-Ru-(\mu-O)-Ru(O^{\bullet})](bpy)_2\}^{4+}$ and $\{\gamma-[(^{\bullet}O)Ru-(\mu-OH)_2-Ru-(O^{\bullet})][SiW_{10}O_{36}]\}^{4-}$, and there is no way to calculate the redox potentials for these two very different systems such that the values can be meaningfully compared. However, geometries of these species presented in Figure 4 clearly show that the Ru=O bonds are stronger in $\{\gamma-[(^{\bullet}O)Ru-(\mu-OH)_2-Ru(O^{\bullet})]-[SiW_{10}O_{36}]\}^{4-}$ than in $\{(bpy)_2[(O^{\bullet})Ru-(\mu-O)-Ru(O^{\bullet})](bpy)_2\}^{4+}$; the calculated Ru=O bond distances are shorter by 0.04 Å in the former complex. Furthermore, these data also show that neither the geometries of the ligands L nor the $\{Ru-(\mu-OH)_2-Ru\}$ and $\{Ru-(\mu-O)-Ru\}$ cores change significantly upon going from reactants to products for either the Ru_2−POM or the "blue-dimer". In contrast, the Ru−L bond distances (i.e., the Ru−L bond strengths) change significantly for L = $(SiW_{10}O_{36})^{4-}$, while these changes are relatively small for L = bpy (except for the Ru−N bond located at the trans position to the oxo-ligand, which is elongated by 0.15 Å). For the Ru_2−POM, the Ru−O(W) bond distances are shortened by ca. 0.05 Å upon going from **1** to **4** (or **IV**), which clearly indicates the stabilization of the $[Ru_2]-(SiW_{10}O_{36})^{4-}$ interaction in complex **4** (or **IV**) as compared to complex **1**; that is, formation of the Ru=O bonds in **4** (or **IV**) initiates the increase in $[Ru_2]-(SiW_{10}O_{36})^{4-}$ interaction. Another factor that stabilizes the $\{[ORu-(\mu-OH)_2-RuO]-(SiW_{10}O_{36})\}^{4-}$ unit in **4** (or **IV**) is two H-bonds between the bridging OH groups and POM-framework oxygens. As was the case in the "blue-dimer", formation of Ru=O bonds destabilizes the Ru---O_{Si} bonds of **4** (or **IV**) located trans to the oxo-ligand. Thus, the calculated large exothermicity of the reaction of O_2 with $\{\gamma-[Ru-(\mu-OH)_2-Ru][SiW_{10}O_{36}]\}^{4-}$, **1**, as compared to that for the "blue-dimer" $\{(bpy)_2[Ru-(\mu-O)-Ru](bpy)_2\}^{4+}$, is not only due to the formation of relatively strong Ru=O bonds in the $\{\gamma-[(^{\bullet}O)Ru-(\mu-OH)_2-Ru(O^{\bullet})][SiW_{10}O_{36}]\}^{4-}$, **4**, product, but also because of stabilization by the $[ORu-(\mu-OH)_2-RuO]---(SiW_{10}O_{36})\}^{4-}$ interaction in **4** relative to reactant **1**. This effect could be attributed to the electron-rich nature (better σ donor and π acceptor) of $[SiW_{10}O_{36}]^{4-}$ as compared to bpy.

IV. Conclusions

From the above presented results, we can draw the following conclusions:

(1) Four-electron oxidation of $\{\gamma-[(H_2O)Ru^{III}-(\mu-OH)_2-Ru^{III}-(H_2O)][SiW_{10}O_{36}]\}^{4-}$, **I(H$_2$O)**, by O_2 is a highly exothermic process and could occur under mild experimental conditions. The first and second 1e-oxidation occur upon the water-to-oxygen substitution, and the proton transfer from the coordinated water molecule to the superoxide (OO^{-}), respectively. The proton transfer from the terminal OH ligand to OOH fragment, in the resulted hydroperoxo−hydroxo intermediate, completes the second 2e-oxidation process. During this reaction, oxidation states of the Ru-centers increase from +3 to +4, and the final product with the $\{Ru(O)-(\mu-OH)_2-Ru(O)\}$ core should be formulated as a complex containing $Ru^{IV}=O^{\bullet}$ units, rather than $Ru^{V}=O$ groups.

(2) The reverse reaction, that is, water oxidation by the complex $\{\gamma\text{-}[(^{\bullet}O)Ru-(\mu\text{-}OH)_2-Ru(O^{\bullet})](H_2O)[SiW_{10}O_{36}]\}^{4-}$, **IV**, is a highly endothermic process and cannot occur. This conclusion is in dramatic contrast with that reported for the "blue-dimer" $\{(bpy)_2[(O^{\bullet})Ru-(\mu\text{-}O)-Ru(O^{\bullet})](bpy)_2\}^{4+}$ intermediate.[39] The observed difference in reactivity of $\{\gamma\text{-}[(^{\bullet}O)Ru-(\mu\text{-}OH)_2-Ru(O^{\bullet})](H_2O)[SiW_{10}O_{36}]\}^{4-}$, **IV**, and $\{(bpy)_2[(O^{\bullet})Ru-(\mu\text{-}O)-Ru(O^{\bullet})](bpy)_2\}^{4+}$ was explained in terms of the electron-rich nature (better σ donor and π acceptor) of $[SiW_{10}O_{36}]^{4-}$ relative to bpy.

Significantly, it is predicted that the lack of reactivity of the intermediate $\{\gamma\text{-}[(^{\bullet}O)Ru-(\mu\text{-}OH)_2-Ru(O^{\bullet})][SiW_{10}O_{36}]\}^{4-}$ toward the water molecule facilitates its complexation with another $\{\gamma\text{-}[Ru^{III}-(\mu\text{-}OH)_2-Ru^{III}][SiW_{10}O_{36}]\}^{4-}$ molecule forming the experimentally[58] isolated and thoroughly characterized water oxidation catalyst $[\{Ru_4O_4(OH)_2(H_2O)_4\}(\gamma\text{-}SiW_{10}O_{36})_2]^{10-}$. Computational studies of the energy and mechanism of this dimerization-like process, **IV** + $[\{Ru^{III}_2(OH)_2\}(\gamma\text{-}SiW_{10}O_{36})]^{4-} \rightarrow [\{Ru_4O_4(OH)_2(H_2O)_4\}(\gamma\text{-}SiW_{10}O_{36})_2]^{10-} + 2H^+$, are in progress.

Acknowledgment. The present research is supported in part by grants DE-FG02-03ER15461 and DE-FG02-07ER15906 of the U.S. Department of Energy. The use of computational resources at the Cherry Emerson Center for Scientific Computation is also acknowledged.

Supporting Information Available: Complete refs 64 and 82, Cartesian coordinates, results of Mulliken analysis, and components of PCM energy for all structures discussed. This material is available free of charge via the Internet at http://pubs.acs.org.

JA900017G